# Heme regulation of human cystathionine β-synthase activity: Insights from fluorescence and Raman spectroscopy

Colin L. Weeks[a], Sangita Singh[b,c], Peter Madzelan[b], Ruma Banerjee[b,c] and Thomas G. Spiro[a]*

*From the [a]Department of Chemistry, University of Washington, Seattle, WA, 98195, [b]Department of Biochemistry, University of Nebraska, Lincoln, NE, 68588-0664 and [c]Department of Biological Chemistry, University of Michigan Medical Center, Ann Arbor, MI, 48109-5606*

## Supporting Information

**Full Reference Details**

30. Kraus, J. P.; Janosik, M.; Kozich, V.; Mandell, R.; Shih, V.; Sperandeo, M. P.; Sebastio, G.; de Franchis, R.; Andria, G.; Kluijtmans, L. A. J.; Blom, H.; Boers, G. H. J.; Gordon, R. B.; Kamoun, P.; Tsai, M. Y.; Kruger, W. D.; Koch, H. G.; Ohura, T.; Gaustadnes, M., *Hum. Mutat.* **1999,** *13*, 362-375.

63. Shintani, T.; Iwabuchi, T.; Soga, T.; Kato, Y.; Yamamoto, T.; Takano, N.; Hishiki, T.; Ueno, Y.; Ikeda, S.; Sakuragawa, T.; Ishikawa, K.; Goda, N.; Kitagawa, Y.; Kajimura, M.; Matsumoto, K.; Suematsu, M., *Hepatology* **2009,** *49*, 141-150.

**Table S1** Frequencies ($cm^{-1}$) and assignment of bands in the resonance Raman spectra of PLP-Tris Schiff base, ferric, ferrous, and heat-inactivated ferrous and CO bound forms of hCBS, ferric, ferrous and CO bound forms of R266M hCBS.

| Assignment | PLP-Tris Schiff base | | hCBS | | | | | | R266M hCBS | | |
|---|---|---|---|---|---|---|---|---|---|---|---|
| | | | Ferric | | Ferrous | | Heat-inactivated ferrous | CO adduct | Ferric | Ferrous | CO adduct |
| | pH 8.6 | pD 8.6 | pH 8.6 | pD 8.6 | pH 8.6 | pD 8.6 | pH 8.5 | pH 8.6 | pH 8.5 | pH 8.5 | pH 8.5 |
| PLP νC=N | 1645 | 1634 | 1665 | 1653 | 1665 | 1653 | | | 1663 | | |
| heme $\nu_{10}$ | | | 1634 | 1633 | | | 1627 | 1632 | 1631 | | 1631 |
| heme $\nu C_a{=}C_b$ | | | 1620 | | 1621 | 1620 | 1618 | 1621 | 1619 | 1620 | 1620 |
| heme $\nu_{37}$ | | | 1605 | 1604 | 1611 | 1608 | 1605 | 1604 | | 1604 | 1603 |
| PLP $\nu_{8a}$ | 1598 | 1603 | | | | | | | | | |
| heme $\nu_2$ | | | 1579 | 1581 | 1583 | 1584 | 1582 | 1584 | 1587 | 1582 | 1583 |
| | | | | | | | | | 1573 | | |
| heme $\nu_{38}$ | | | 1556 | 1558 | 1554 | 1559 | 1556 | 1562 | 1551 | 1553 | 1556 |
| PLP $\nu_{8b}$ | 1539 | | | | | | | | | | |
| heme $\nu_{11}$ | | | 1535 | | 1535 | | 1535 | | | | |
| | | 1520 | | | | | | | | | |
| | | | | | 1515 | 1518 | | | | | |
| heme $\nu_3$ | | | 1500 | 1502 | 1492 | 1492 | 1492 | 1497 | 1499 | 1491 | 1497 |
| PLP $\nu_{19a}$ | 1467 | 1471 | | | | | | | | | |
| | | | 1466 | 1467 | 1469 | 1470 | 1471 | 1469 | 1468 | 1470 | 1465 |
| heme $\delta_s(=CH_2)$ | | | 1437 | 1437 | 1433 | 1430 | 1429 | 1431 | 1434 | 1430 | 1431 |
| | | | | | 1420 | | | | | | |
| PLP $\nu_{14}$ | 1396 | | | | | | | | | | |
| heme $\nu_{12}$ | | | 1394 | | | 1386 | 1388 | 1387 | 1391 | 1388 | 1386 |
| heme $\nu_4$ | | | 1372 | 1372 | 1357 | 1357 | 1360 | 1372 | 1372 | 1359 | 1371 |
| | 1364 | 1369 | | | | | | | | | |

| | | | | | | | | | | | |
|---|---|---|---|---|---|---|---|---|---|---|---|
| PLP νC–O | 1342 | 1341 | 1338 | 1340 | 1338 | 1340 | 1339 | 1339 | 1337 | 1336 | |
| heme δ($C_aH$) | | | 1315 | 1311 | 1314 | 1314 | 1310 | 1305 | 1312 | | 1305 |
| PLP $\nu C_4–C_4'$ | 1309 | 1310 | | | | | | | | | |
| | | | 1217 | 1215 | | | 1228 | 1226 | 1217 | 1223 | 1225 |
| PLP $\nu_{9a}$ | 1191 | 1185 | | | | | | | | | |
| heme $\nu_{30}$ | | | 1174 | 1177 | | | 1170 | 1169 | 1171 | 1169 | 1171 |
| | | | | | | | 1128 | 1131 | 1119 | | 1120 |

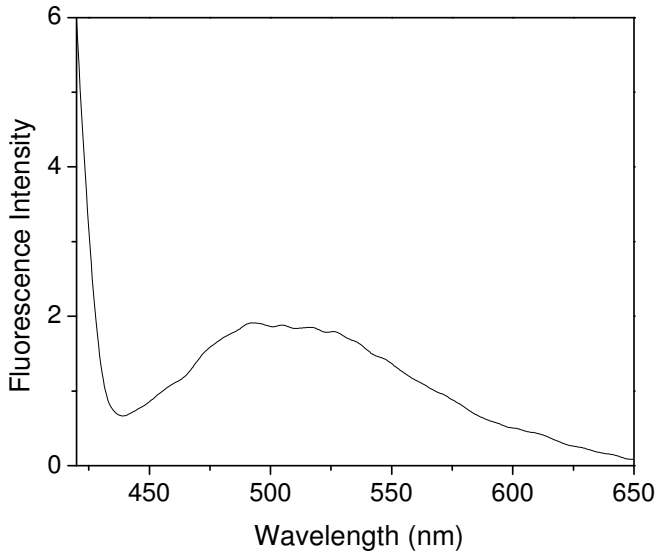


**Figure S1**. Fluorescence emission spectrum of PLP (106 μM) in Tris buffer (pH 8.5, 100 mM). Excitation wavelength, 410 nm.

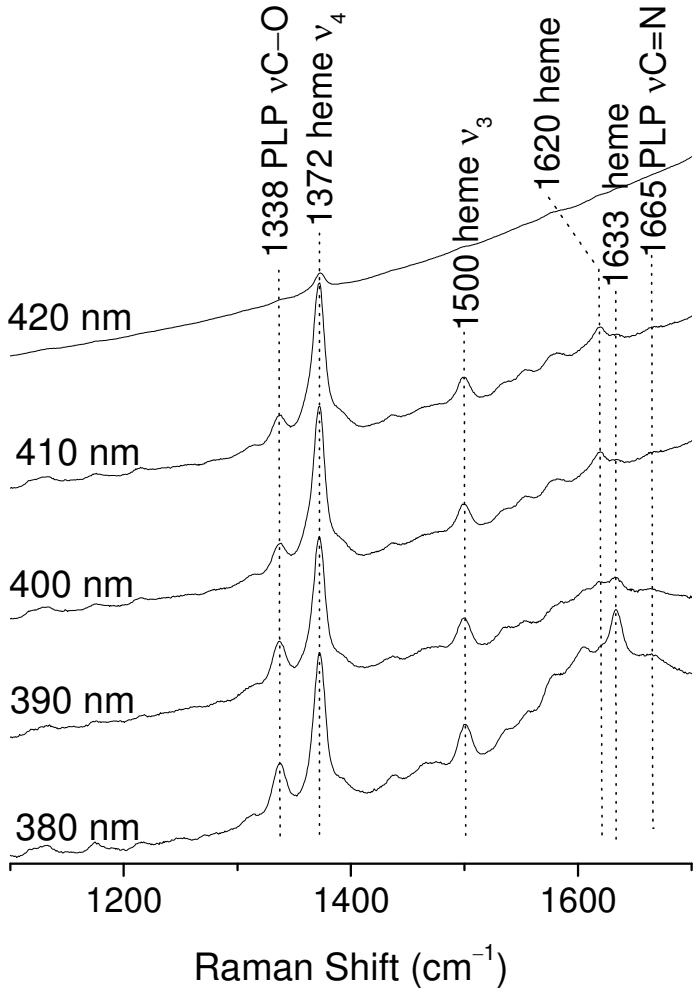


**Figure S2**. Raman spectra of ferric hCBS in Tris buffer pH 8.6 recorded using excitation wavelengths from 380-420 nm. Accumulation time, 15 min.

Though the heme modes of hCBS were the most intense Raman bands at all excitation wavelengths (380-420 nm), the relative enhancement of the PLP modes increased as the excitation wavelength became shorter, with the additional advantage that the fluorescence background was reduced at shorter excitation wavelengths. This was because the maximum absorption for the PLP Schiff base, 412 nm in the resting state, is at a shorter wavelength than the heme Soret band at 429 nm and 449 nm in the ferric and ferrous states, respectively.

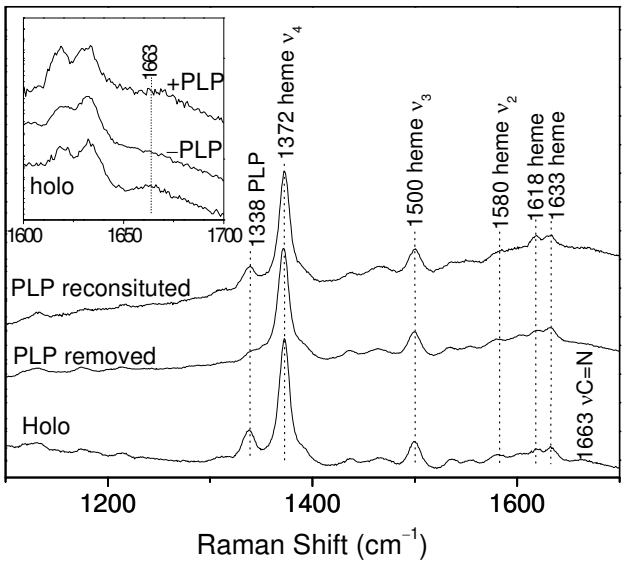


**Figure S3.** Raman spectra of Fe(III)hCBS before and after PLP removal by washing with serine and apo-Fe(III)hCBS reconstituted with PLP in 50 mM Tris buffer pH 8.6. Excitation wavelength, 390 nm. Accumulation time, 30 min.

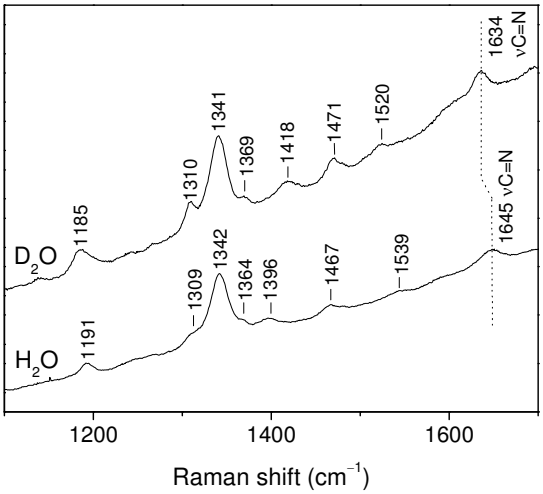


**Figure S4**. Raman spectra of the PLP-Tris Schiff base at pH (pD) 8.6 in $H_2O$ and $D_2O$. Excitation wavelength, 390 nm. Accumulation time, 15 min.

The aldehyde group of PLP reacts with the amine of Tris [tris(hydroxymethl)aminomethane] to form a Schiff base adduct in aqueous solution. Raman spectra were recorded of the PLP-Tris Schiff base as a control to check that signals from PLP in the Raman spectra of hCBS in Tris buffer solutions were coming from PLP bound to hCBS and not PLP that had been released from the protein and reacted with the buffer. The $D_2O$ experiment was also done to demonstrate the shift in the νC=N band upon deuteration of the PLP-Schiff base.

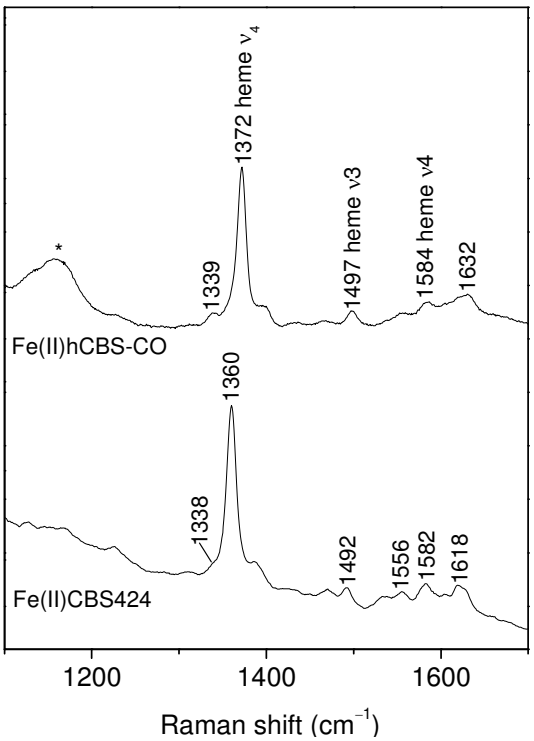


**Figure S5.** Raman spectra of Fe(II)CBS424 and Fe(II)hCBS-CO formed from Fe(II)hCBS 20 min after the initiation of CO binding ($\lambda_{ex}$ = 390 nm) in 100 mM Tris buffer pH 8.6. Accumulation time, 10 min. *Peak arising from the reductant, dithionite.

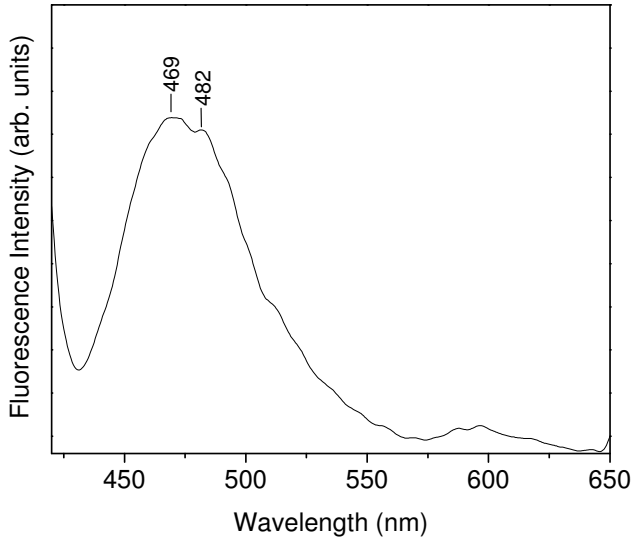


**Figure S6**. Fluorescence spectrum 23 h after initiation of CO binding to Fe(II)CBS (36 μM) in 100 mM phosphate buffer pH 8.0. 410 nm excitation spectrum.

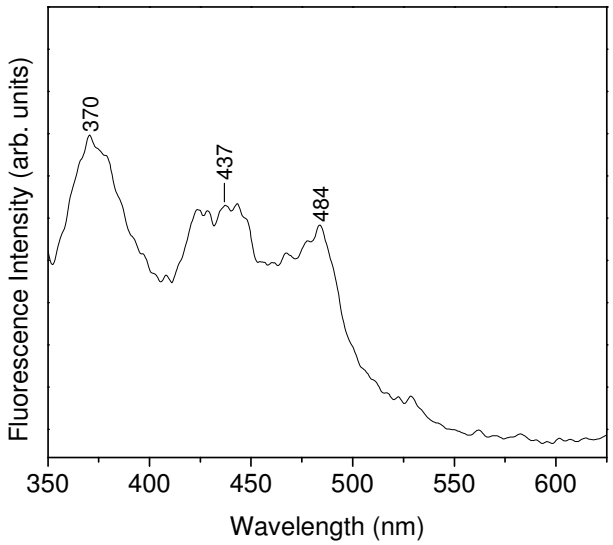


**Figure S7**. Fluorescence emission spectrum of PLP (106 μM) in Tris buffer (pH 8.5, 100 mM). Excitation wavelength, 330 nm.

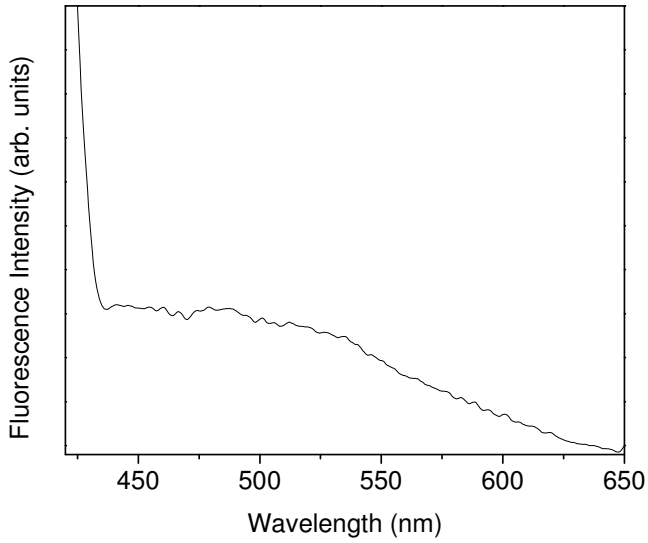


**Figure S8**. Fluorescence emission spectrum of PLP (50 μM) in phosphate buffer (pH 8.0, 100 mM). Excitation wavelength, 410 nm.

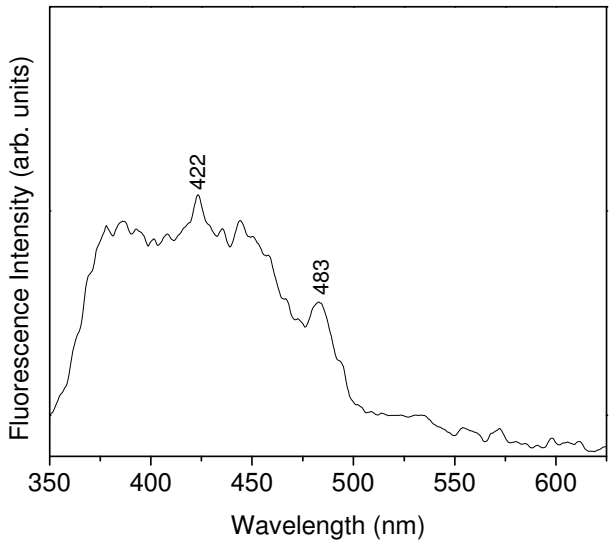


**Figure S9**. Fluorescence emission spectrum of PLP (50 μM) in phosphate buffer (pH 8.0, 100 mM). Excitation wavelength, 330 nm.

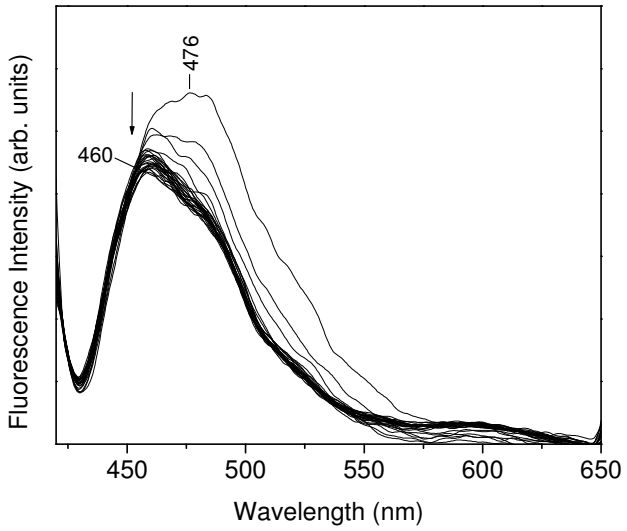


**Figure S10**. Time dependence of fluorescence spectra after CO binding to Fe(II)hCBS (30 μM) in 5.0 mM phosphate buffer pH 8.0. 410 nm excitation spectra were collected every 10 min for 4 h.

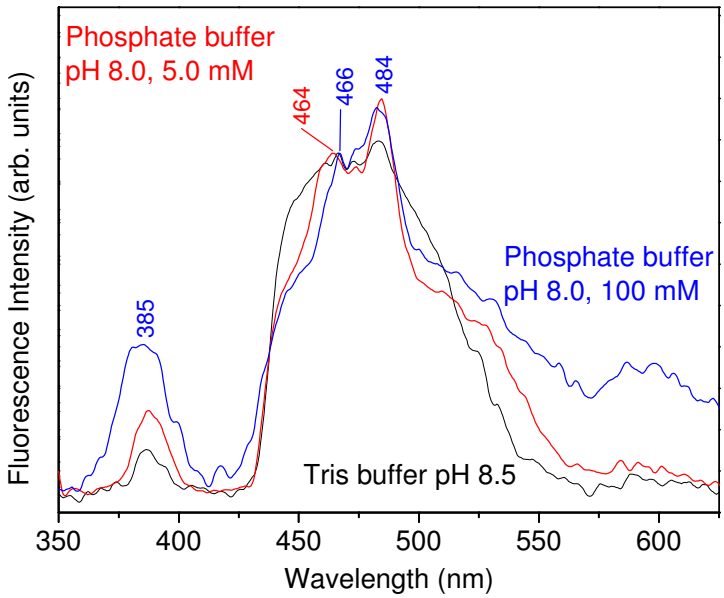


**Figure S11**. Fluorescence spectra measured 5-6 h after CO binding to Fe(II)hCBS in Tris buffer 100 mM, pH 8.5; phosphate buffer 100 mM, pH 8.0; and phosphate buffer 5.0 mM, pH 8.0. 330 nm excitation.

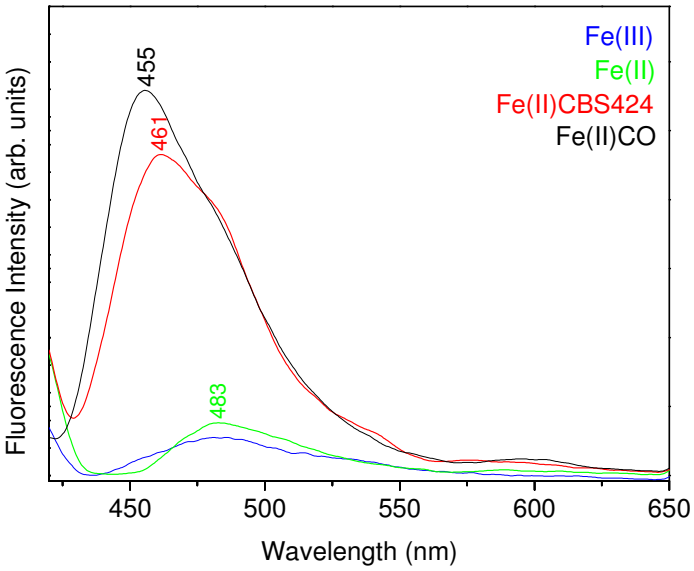


**Figure S12**. Fluorescence emission spectra of the indicated forms of hCBS in Tris buffer 100mM. pH 8.5. [hCBS] = 48 μM. 410 nm excitation spectra.

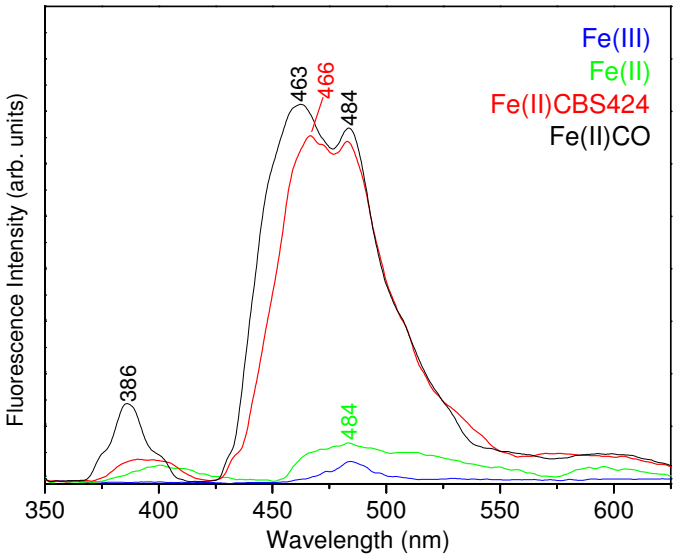


**Figure S13**. Fluorescence emission spectra of the indicated forms of hCBS in Tris buffer pH 8.5, [hCBS] = 48 μM. 330 nm excitation spectra.

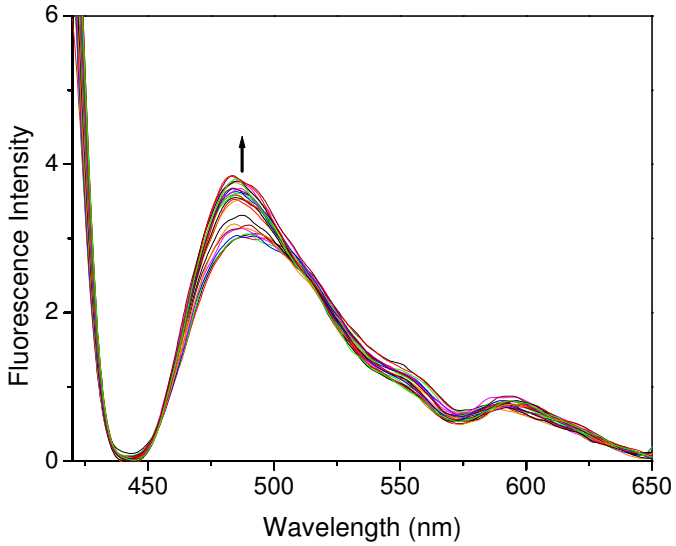


**Figure S14**. Time dependence of fluorescence emission spectra of Fe(II)hCBS (31 μM) in Tris buffer pH 8.5. Excitation wavelength: 410 nm. Spectra were collected at 10 min intervals for 4 h.

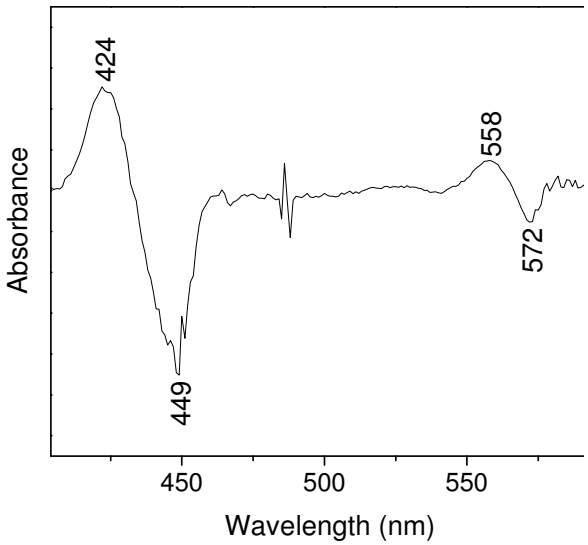


**Figure S15**. UV-vis absorption difference spectrum of the ferrous hCBS in Tris buffer pH 8.5 of sample used to record the time-dependent fluorescence measurements. The spectrum recorded prior to the fluorescence measurements was subtracted from the spectrum recorded after completion of the fluorescence measurements.

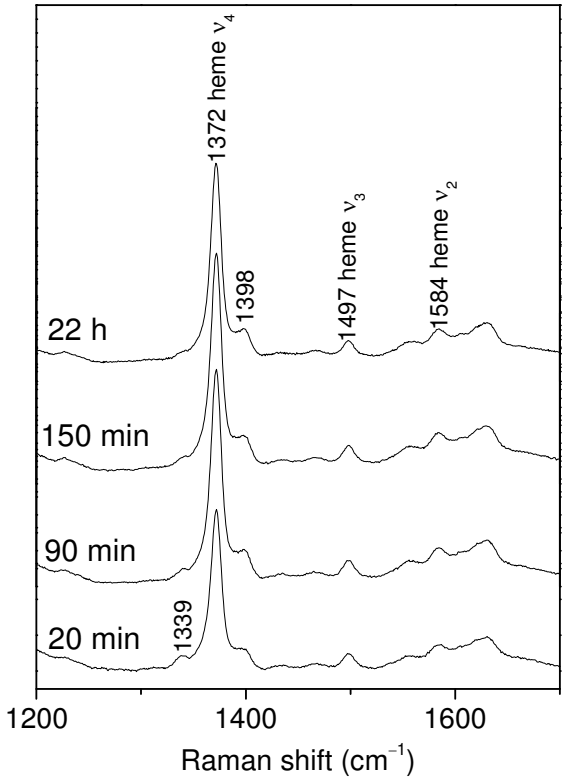


**Figure S16.** Raman spectra of hCBS-CO formed from Fe(II)hCBS in Tris buffer pH 8.6 at the indicated time points after the start of CO binding. $\lambda_{ex}$=390 nm. Accumulation time, 10 min.

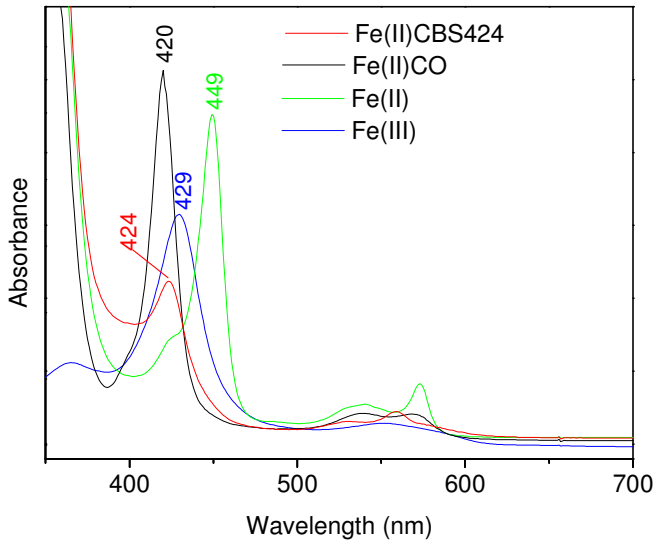


**Figure S17**. Electronic absorption spectra of the indicated forms of hCBS in Tris buffer pH 8.5.

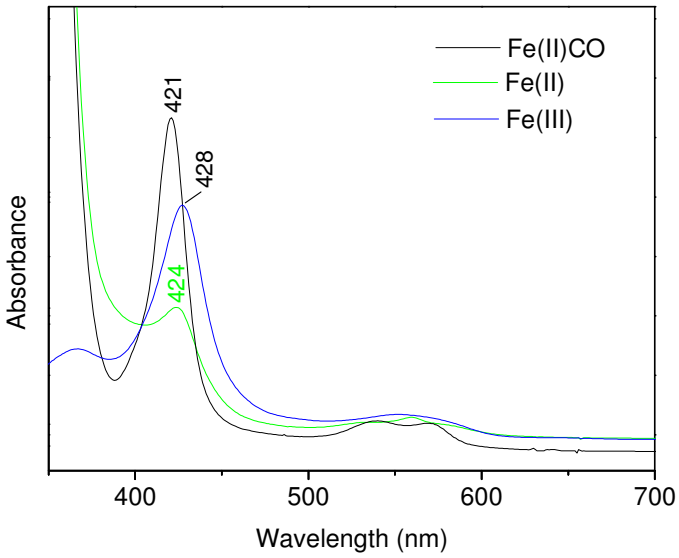


**Figure S18**. Electronic absorption spectra of the indicated forms of R266M hCBS in phosphate buffer pH 8.0.